Simulation of the Propagation and Diffusion of Dark Atoms in the Earth's Surface

Kharakhashyan Artem

Research Institute of Physics, Southern Federal University,

Rostov-on-Don, Russia

28th International Workshop
''What comes beyond the standard models''

2025

Outline

- Introduction
- Necessary estimates of the properties of the Dark Atom
- Effects of Directionality and Obstruction on the detection of Dark Matter particles
- Beam Approximation and the Simulation Framework description
- Quantitative Estimates
- Qualitive Estimates
- Spatial Distribution
- Conclusions

Underground Detectors

- Over many decades of research, a wide range of robust and theoretically well-founded models of Dark Matter have been proposed.
- Consequently, experimental verification of the proposed dark matter candidates has become a priority.
- Explanation of DAMA/LIBRA results assume annual modulation of low energy binding of dark atoms with nuclei.
- The obtained results enable, on the one hand, to analyze the expectations for various models, and on the other hand, to explain the observational results themselves, using these models – specifically, in terms of dark atoms having strong interactions with matter.

Purpose

- The long-standing results of the DAMA/NaI and DAMA/LIBRA experiments [1, 2, 3], based on the model-independent observation of Dark Matter annual modulation, are examined here within the framework of the Dark Atom model.

- Specifically, the model proposes that dark atoms are captured by the Earth, leading to an annual modulation in their concentration within the detector material. These dark atoms may then bind to sodium or iodine nuclei at energy levels of a few keV. In this context, we present basic theoretical considerations and provide quantitative and qualitive estimates about this hypothesis.

- We present a framework developed for modeling the propagation and diffusion processes, and calculating the concentration of dark matter particles within the Earth's surface layers, as well as for performing detection with underground detectors. The developed framework accounts for the Earth's orientation relative to the dark matter halo, the velocities and directions of motion of the Solar System and the Earth relative to the galactic center, the relief of the Earth's surface, the geometry of the detector, and the directions of particle arrival at the Earth's surface.

Dark Atoms

- When primordial helium is formed in Big Bang nucleosynthesis, the excessive $-2n$ charged particles bind to the n nuclei of primordial helium-4 — this is the way to form of Thompson type dark atoms. They are $n-\alpha$-particle nuclei with electric charge compensated by superheavy $-2n$ charged lepton inside them.

- Dark atoms have strong (nuclear) elastic cross section of interaction with protons and nuclei, however the inelastic process of their radiative capture is strongly suppressed [M. Y. Khlopov, A. G. Mayorov, and E. Y. Soldatov. Composite dark matter and puzzles of dark matter searches. International Journal of Modern Physics D, 19(08n10):1385–1395, 2010.].

- Most of restrictions can not be applied to dark atom scenario and describe the point-like particles elastic scattering only.

- It can provide a solution for the problem of anomalous isotope production by capture of protons and helium in the dark-atom formation period.

Necessary estimates of the properties of the dark atom

Cross section of dark atom interactions

- For nuclear interaction cross section $\sigma \sim 10^{-25} \mathrm{cm}^2$ and the averaged number density $\sim n$, dark atoms appear as collisionless gas at the scale of Galaxy. At the average baryonic number density, the Galaxy is also transparent for dark atoms.

$$m \sim 1 - 10\, TeV$$

- However, baryonic clouds or objects with the size $\sim R$ and baryon number density $n \sim 10^{-4} (1\,\mathrm{TeV}/m) \mathrm{cm}^{-3}$, satisfying the condition $n\sigma R > 1$ are opaque for dark atoms, and capture them if $n\sigma (m_p/m) R > 1$.

- The rate of radiative capture of dark atom by nuclei can be estimated with the use of the analogy with the radiative capture of a neutron by a proton:

$$\sigma v = \frac{f\pi\alpha}{m_p^2} \frac{3}{\sqrt{2}} \left(\frac{Z}{A}\right)^2 \frac{T}{\sqrt{A m_p E}}$$

Necessary estimates of the properties of the dark atom

Cross section of dark atom interactions

- Using for the initial estimation $f = 1.4 \cdot 10^{-3}, E = 4\ \mathrm{KeV}$ and the detector temperature $T = 300\ \mathrm{K}$ it can be calculated, that:

$$\langle \sigma v \rangle_{Na} \approx 4.9 \cdot 10^{-20} \mathrm{MeV}^{-2} = 5.9 \cdot 10^{-31}\ \mathrm{cm}^3/\mathrm{s}$$

$$\langle \sigma v \rangle_{I} \approx 1.6 \cdot 10^{-20} \mathrm{MeV}^{-2} = 1.9 \cdot 10^{-31}\ \mathrm{cm}^3/\mathrm{s}$$

- To obtain pure cross sections, it is necessary to divide these values by the thermal velocity of the nucleus:

$$v_i = \sqrt{\frac{3T}{m_i}}$$

Necessary estimates of the properties of the dark atom

Drift Velocity and Underground Concentration

- The average dark atom concentration and flow velocity around around the NaI(Tl) detectors of the DAMA experiments can be quantitatively estimated. The continuity equation in the case considered can be given as follows[5]:

$$n_0 V_h = n V_{drift} \qquad V_{drift} = \frac{3T}{m^2 n_{gr} \langle \sigma_t v^3 \rangle} M_O g$$

- Here V_{drift} is a velocity of the dark atoms drift deeply into the Earth under the influence of gravity after thermalization.

- The average mass of ground particles m and their concentration n_{gr} can be estimated for silicates SiO_2, for example.

- The $\langle \sigma_t v^3 \rangle$ is the averaged by the Maxwellian distribution, and the transport cross section can be approximated $\sigma_t \sim A^{2/3} \frac{m}{M_O} \sigma_{nuclear}$ The concentration $n \sim 1\ \mathrm{cm}^{-3}$

Effects of Directionality and Obstruction on the detection of Dark Matter particles

- The detection process is influenced by many factors, such as topography, detector depth, detector geometry, position and orientation of the Earth relative to dark matter halo.
- The Earth may act as an obstacle to the flow of dark atoms.
- Flux through the Earth's surface is influenced by relative velocities and is modulated by their changes.

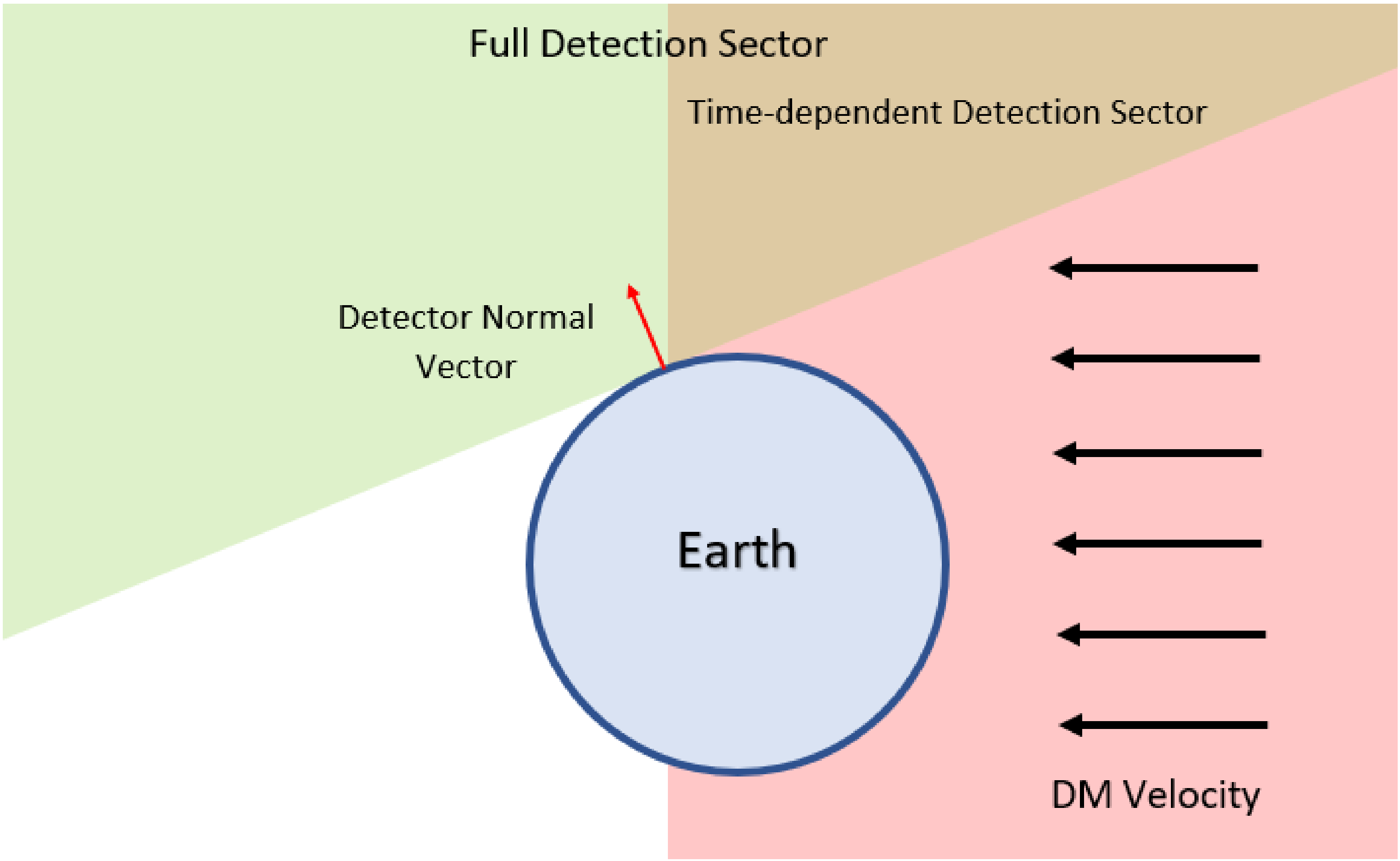

Schematic representation of the effects of directionality and obstruction on the detection of Dark Matter particles.

Topographic Map

- NASA's topographic map can be used to reconstruct the 3D structure of the Earth's surface and assess the effect of terrain roughness on particle dispersion and the resulting impact on concentration over time.

https://visibleearth.nasa.gov/images/73934/topography

- It provides information both about the natural obstacles themselves and about the length of the path that particles must travel to reach the detector.

3D Map of Area of Interest

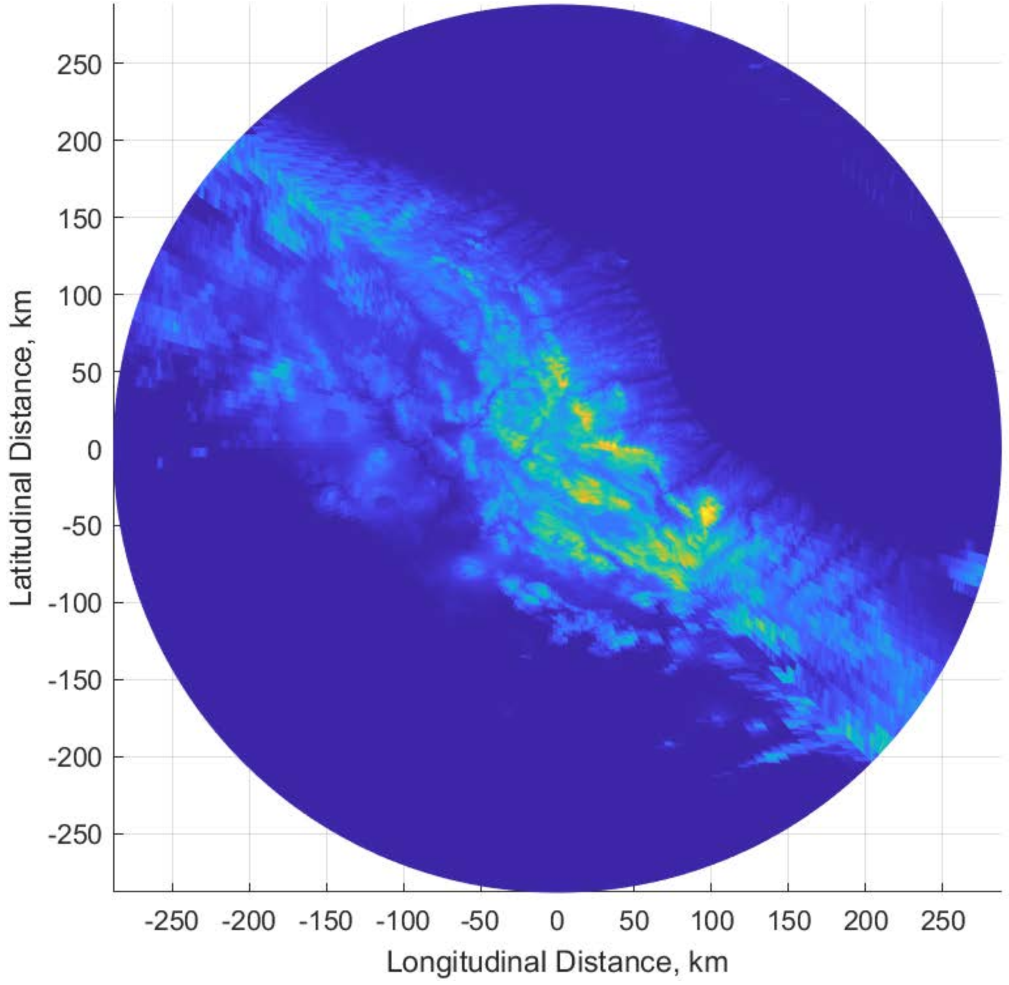

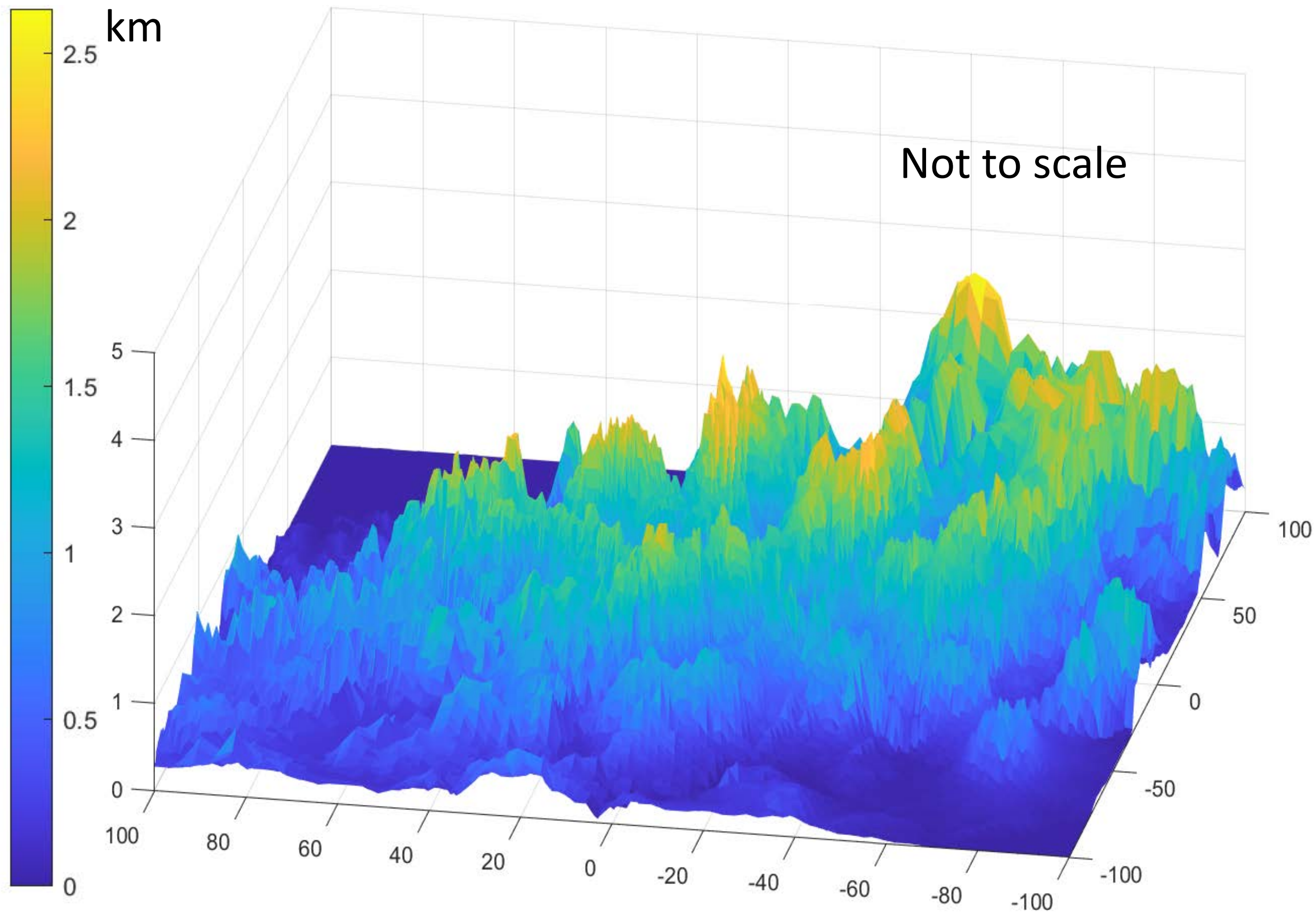

A three-dimensional reconstruction of the area around the detector.
Many potential obstacles in the form of mountain peaks can be seen.

Beam Approximation

- The flow of dark atoms is considered as a set of propagating beams, which, upon collision with the Earth's surface, slow down and undergo a thermalization process.
- The intensity of each beam along its propagation path is calculated using the modified Beer-Lambert's law.
- Each beam specifies the potential direction of arrival of the flow of dark atoms from space in the upper region of the half-space, relative to the horizon.
- The direction of each beam is specified by a directional vector $\overline{d}_{beam}$
- The flux itself is modulated by the total value of the velocity from various sources, as well as by the orientation of the beam in relation to the velocity vector.

$$\overline{V}_{full}(t)$$

Spherical Coordinates and Detector Coordinate System

- The directional vectors $\bar{d}_{beam}$ of the beams are defined in the spherical coordinate system centered on the detector. This reference system is then related to the geodetic coordinate system (latitude, longitude, altitude).

- The azimuthal angle φ is measured counterclockwise from the east direction along the longitude axis of the geodetic coordinate system.

- The polar angle θ is measured from the normal vector to the Earth's surface.

- For convenience, the beams are numbered starting from the azimuthal axis:

$$\theta_{beam} = \frac{\pi}{2} - \theta$$

- Radial distance is the length of the beam.

Points of intersection of beams with the Earth's surface

- For each azimuthal angle, there is a half-plane passing through the normal vector to the Earth's surface and the direction vector of each ray with the same angle.
- This half-plane is perpendicular to the azimuthal plane.
- For each such half-plane, we calculate the intersection points between the two dimensional interpolated topographic approximation of the Earth's surface and the linear segments defined by the directional vectors.
- The first point of each segment is at the detector, and the second point lies on the surface of a semi-sphere of radius R = 288 km, which covers the entire area of interest.

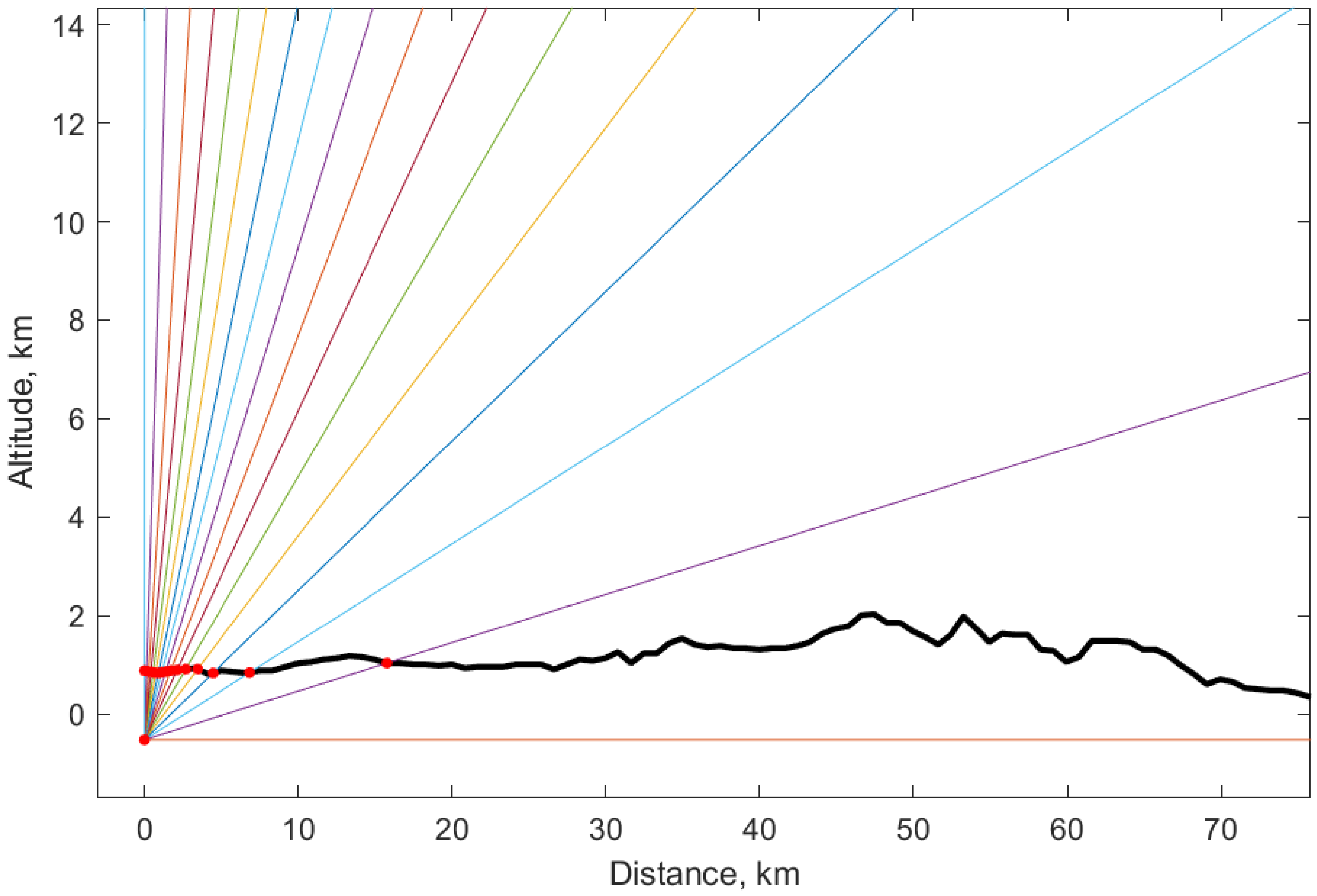

Technical Details

- Frameworks consists of two programs in MATLAB and Python AstroPy.
- Ephemerides data was used to calculate exact positions and velocities with reference to specific time.
- The DAMA detector is located underground at the Laboratori Nazionali del Gran Sasso, which is shielded by about 1400 meters of rock, corresponding to approximately 3400 meters water equivalent of overburden.
- Following coordinate systems were used:
  - Detector coordinate system (detector-centered rectangular)
  - Spherical coordinate system (detector-centered spherical, for beams)
  - Geodetic coordinate system
  - Geocentric Celestial Reference System (GCRS)
  - Galactocentric reference frame

Coordinates of **Laboratori Nazionali del Gran Sasso**

latitude longitude
42°25′16″N 13°30′59″E or **42.42111°N, 13.51639°E**

International Celestial Reference System (ICRS) Geocentric Celestial Reference System (GCRS)

- The International Celestial Reference System (ICRS) is the fundamental celestial reference system adopted by the International Astronomical Union (IAU) for high-precision positional astronomy. The ICRS, with its origin at the solar system barycenter and "space fixed" axis directions, is meant to represent the most appropriate coordinate system for expressing reference data on the positions and motions of celestial objects.
- Orientation:

  Principal plain (δ = 0): true celestial equator at epoch J2000.0 given through the precession and nutation models.
- Origin of right ascension (α = 0):

  Ascending intersection point (Aries) between the equatorial and the mean ecliptical plains.
- GCRS is similar to ICRS, but it is relative to the Earth's center-of-mass rather than the Solar System Barycenter.

Galactocentric Reference Frame

Right Ascension, Declination, and heliocentric distance from ICRS to Cartesian:

$$x_{\mathrm{icrs}} = d\cos\alpha\cos\delta$$
$$y_{\mathrm{icrs}} = d\sin\alpha\cos\delta$$
$$z_{\mathrm{icrs}} = d\sin\delta$$
$$\boldsymbol{r}_{\mathrm{icrs}} = \begin{pmatrix} x_{\mathrm{icrs}} \\ y_{\mathrm{icrs}} \\ z_{\mathrm{icrs}} \end{pmatrix}$$

Rotation matrices:

$$\boldsymbol{R}_1 = \begin{bmatrix} \cos\delta_{\mathrm{GC}} & 0 & \sin\delta_{\mathrm{GC}} \\ 0 & 1 & 0 \\ -\sin\delta_{\mathrm{GC}} & 0 & \cos\delta_{\mathrm{GC}} \end{bmatrix}$$

$$\boldsymbol{R}_2 = \begin{bmatrix} \cos\alpha_{\mathrm{GC}} & \sin\alpha_{\mathrm{GC}} & 0 \\ -\sin\alpha_{\mathrm{GC}} & \cos\alpha_{\mathrm{GC}} & 0 \\ 0 & 0 & 1 \end{bmatrix}.$$

$$\eta = 58.5986320306^\circ$$

$$\boldsymbol{R}_3 = \begin{bmatrix} 1 & 0 & 0 \\ 0 & \cos\eta & \sin\eta \\ 0 & -\sin\eta & \cos\eta \end{bmatrix}$$

$$\boldsymbol{R} = \boldsymbol{R}_3\boldsymbol{R}_1\boldsymbol{R}_2 =$$
$$\begin{bmatrix} \cos\alpha_{\mathrm{GC}}\cos\delta_{\mathrm{GC}} & \cos\delta_{\mathrm{GC}}\sin\alpha_{\mathrm{GC}} & -\sin\delta_{\mathrm{GC}} \\ \cos\alpha_{\mathrm{GC}}\sin\delta_{\mathrm{GC}}\sin\eta - \sin\alpha_{\mathrm{GC}}\cos\eta & \sin\alpha_{\mathrm{GC}}\sin\delta_{\mathrm{GC}}\sin\eta + \cos\alpha_{\mathrm{GC}}\cos\eta & \cos\delta_{\mathrm{GC}}\sin\eta \\ \cos\alpha_{\mathrm{GC}}\sin\delta_{\mathrm{GC}}\cos\eta + \sin\alpha_{\mathrm{GC}}\sin\eta & \sin\alpha_{\mathrm{GC}}\sin\delta_{\mathrm{GC}}\cos\eta - \cos\alpha_{\mathrm{GC}}\sin\eta & \cos\delta_{\mathrm{GC}}\cos\eta \end{bmatrix}$$

Position transformation:

$$\hat{\boldsymbol{x}}_{\mathrm{GC}} = (1,0,0)^{\mathsf{T}}.$$

$$\boldsymbol{r}' = \boldsymbol{R}\boldsymbol{r}_{\mathrm{icrs}} - d_{\mathrm{GC}}\hat{\boldsymbol{x}}_{\mathrm{GC}}.$$

Height of the Sun above the Galactic midplane correction:

$$\theta = \sin^{-1}(z_\odot/d_{\mathrm{GC}})$$

$$\boldsymbol{H} = \begin{bmatrix} \cos\theta & 0 & \sin\theta \\ 0 & 1 & 0 \\ -\sin\theta & 0 & \cos\theta \end{bmatrix}$$

Finally:

$$\boldsymbol{r}_{\mathrm{GC}} = \boldsymbol{H}\left(\boldsymbol{R}\boldsymbol{r}_{\mathrm{icrs}} - d_{\mathrm{GC}}\hat{\boldsymbol{x}}_{\mathrm{GC}}\right).$$

Coordinate Systems Transformations

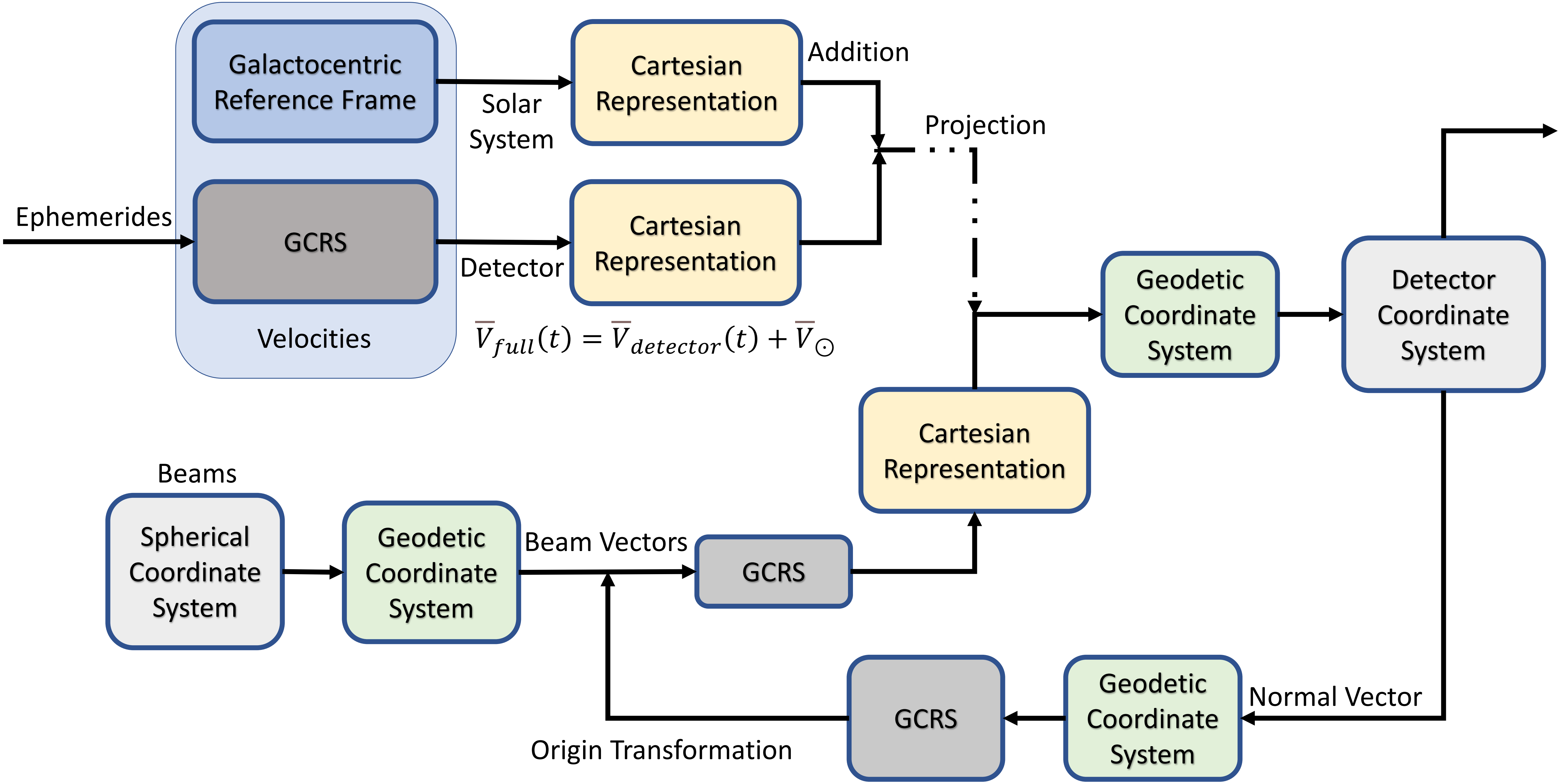

Beer-Lambert's Law

- The intensity of each beam along its propagation path is calculated using the Beer-Lambert's law:

$$I(\varphi, \theta_{beam}, d, t) = I_0(\varphi, \theta_{beam}, t) \cdot e^{-\frac{d}{l}}$$

d is the distance traveled by the beam

l is the mean free path

$$I_0(\varphi, \theta_{beam}, t) = n_{beam} \cdot V_{beam}(t) \cdot S_{\theta_{beam},\varphi}$$

$$V_{beam}(t) = \left|\overline{V}_{full}(t)\right| \cdot \cos\left(\overline{d}_{beam}, \overline{V}_{full}(t)\right)$$

- The analogy of optical propagation of beams with attenuation is used.

- The surface area of the solid angle is bounded by 4 neighboring beams forming a polygon can be calculated as follows:

$$S_{i,j} = R^2 \cdot \frac{2\pi}{n_\varphi}\left(sin\frac{(i+1)\pi}{2n_\theta} - sin\frac{i\pi}{2n_\theta}\right)$$

Drift and Velocity Distribution

- At a depth of about 100 meters, the flow of particles is thermalized, and the process of diffusion towards the center of the Earth begins.
- The direction of the flow changes, and the directional vector of the beam is pointed towards the center of the Earth.
- The points of intersection of the beams with the Earth's surface are used to determine the starting points of the diffusion process.

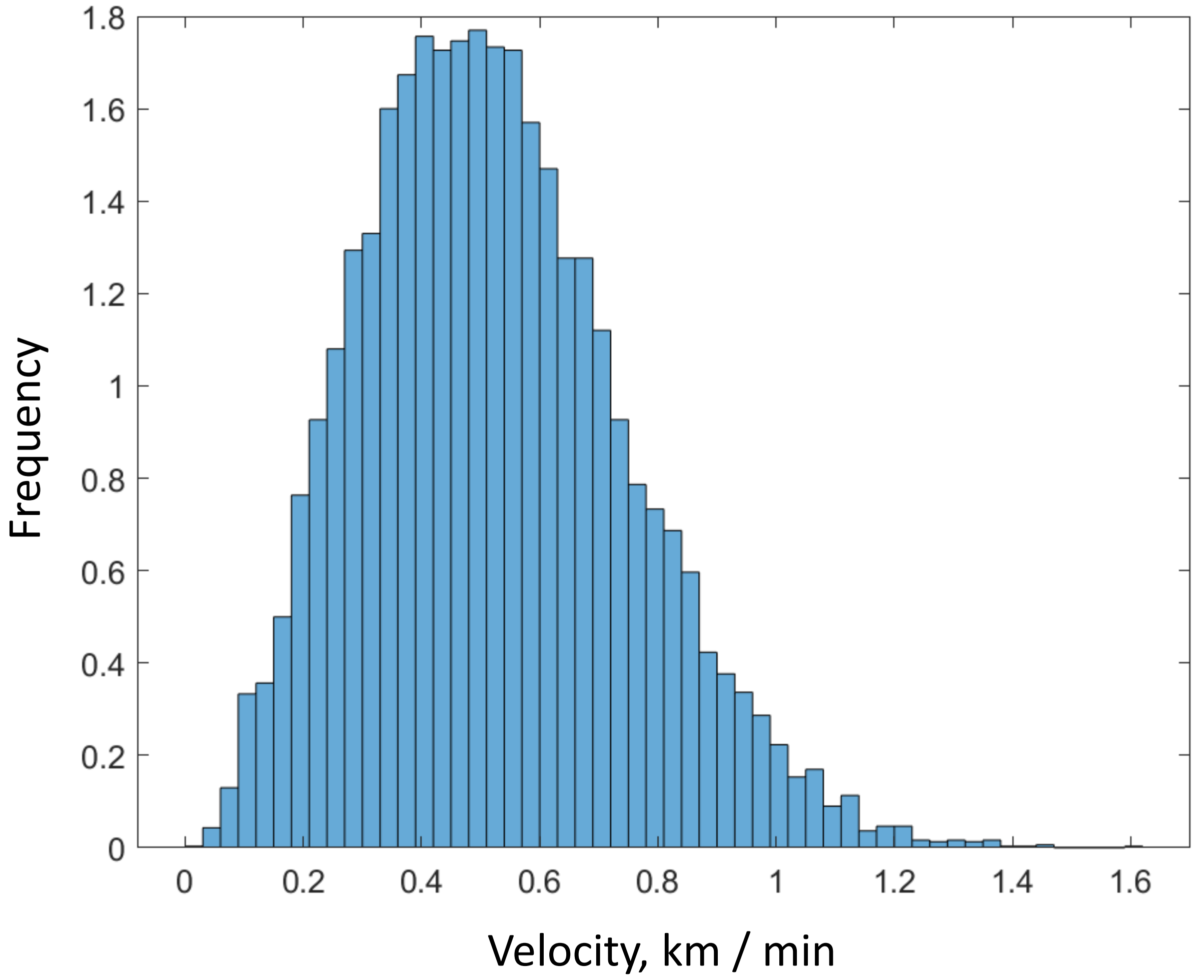

Drift and Velocity Distribution

- Assuming the particle beam moves in the -Z direction toward the Earth's center, the drift directional vector

$$\overline{V}_{drift} = (0, 0, -1)$$

- The particle velocity distribution is given by the Maxwell–Boltzmann distribution with the mean $\approx V_{drift}$

$$f(p) = \sqrt{\frac{2}{\pi}\frac{p^2}{a^3}}\, e^{-\frac{p^2}{2a^2}} \qquad V_{drift} \approx 10^3\ \mathrm{cm/s}$$

- For a set of *p* particles:

$$\overline{V}_p^T \times \overline{V}_{drift}$$

where $\overline{V}_p^T$ is sampled from the Maxwell–Boltzmann distribution above.

Brownian Motion with Drift

$$\boldsymbol{BP}(x,y,z,t) = \sigma_{BM}^2 \boldsymbol{BM}(x,y,z,t) + \overline{V}_p^T \times \overline{V}_{drift} \cdot t$$

$$\sigma_{BM}^2 = 1$$

- Wiener process (by definition)
  - $W_0 = 0$
  - W_t is almost surely continuous
  - $W_t - W_s \sim \mathcal{N}(0, t-s)$ $\quad 0 \leq s \leq t$
- Correlation Matrix for a beam slice, perpendicular to propagation direction $C(t) = \begin{pmatrix} t & 0 & 0 \\ 0 & t & 0 \\ 0 & 0 & \approx 0 \end{pmatrix}$

- The resulting dark atom concentration at time *t* can be estimated as the number of particles inside the detector, divided by the volume of the detector: $n(t) = \dfrac{N_p(t)}{Vol}$

$N_T = 4.015 \cdot 10^{24}$ nuclei / kg $\quad M_O = 2\,TeV$

- **Count rate** can be estimated as $R = \varepsilon \dfrac{n(t)}{M_O}(\langle\sigma v\rangle_{Na} + \langle\sigma v\rangle_I)N_T$

RESULTS

Quantitative Estimates

- Using the equation from M. Y. Khlopov, A. G. Mayorov, and E. Y. Soldatov. Composite dark matter and puzzles of dark matter searches. International Journal of Modern Physics D, 19(08n10):1385–1395, 2010., the **initial estimation** of capture rate can be calculated:

Simulation

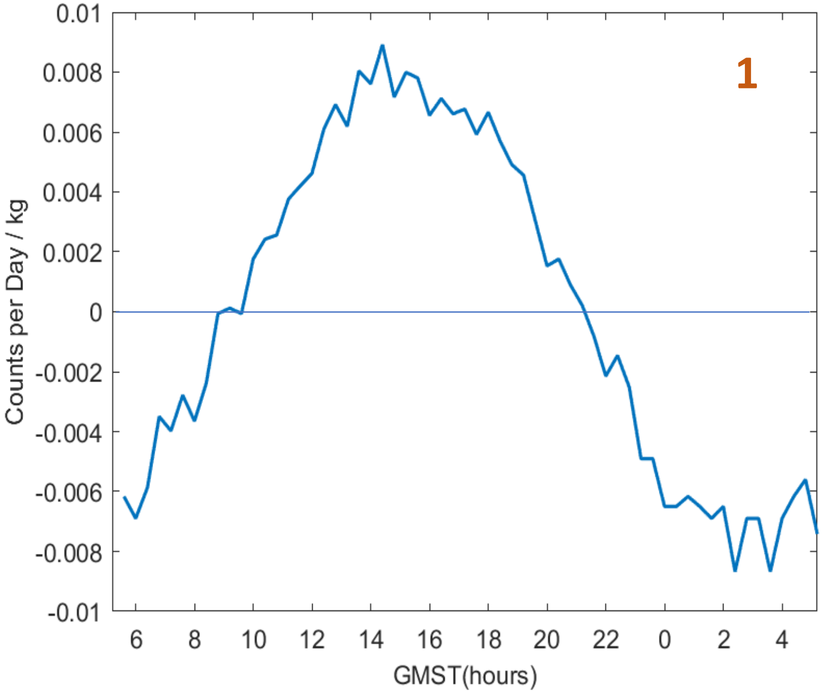

Experiment

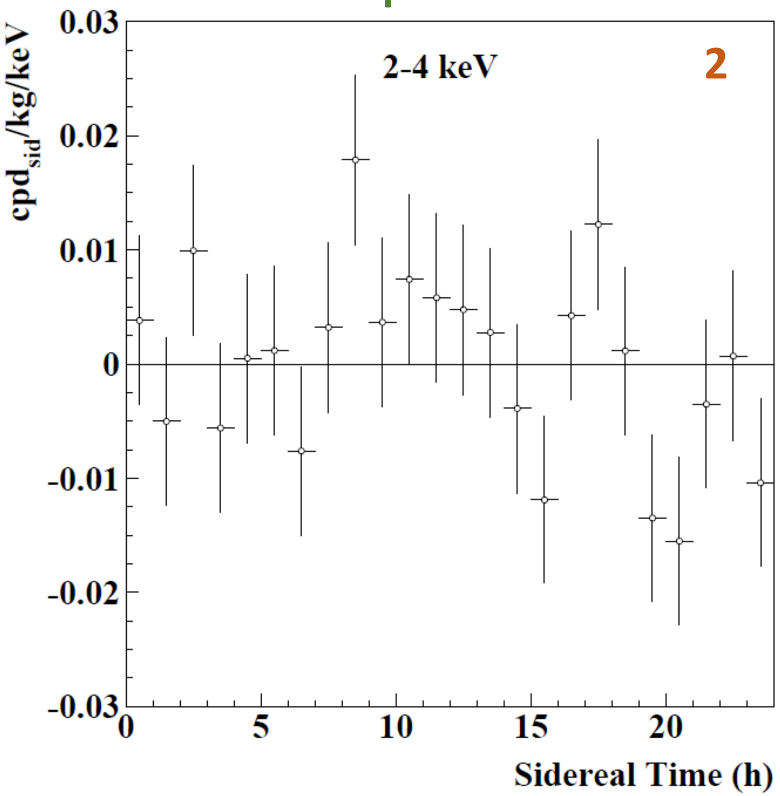

Fig.2. from Bernabei, R., Belli, P., Cappella, F. et al. Model independent result on possible diurnal effect in DAMA/LIBRA-phase1. Eur. Phys. J. C 74, 2827 (2014).

$$R \approx 2.951 \cdot 10^{-6} + 2.011 \cdot 10^{-7} \cos\left(\omega(t - t_0)\right) \text{ counts/s} \cdot \text{kg} =$$

$$= 0.255 + 0.017 \cos\left(\omega(t - t_0)\right) \text{ counts/day} \cdot \text{kg}$$

- The values are close to those required by the experimental data.

Qualitive Estimates

- Identical daily and annual modulation phases
- Cosine dynamics of residuals
- Similar Variance

Simulation

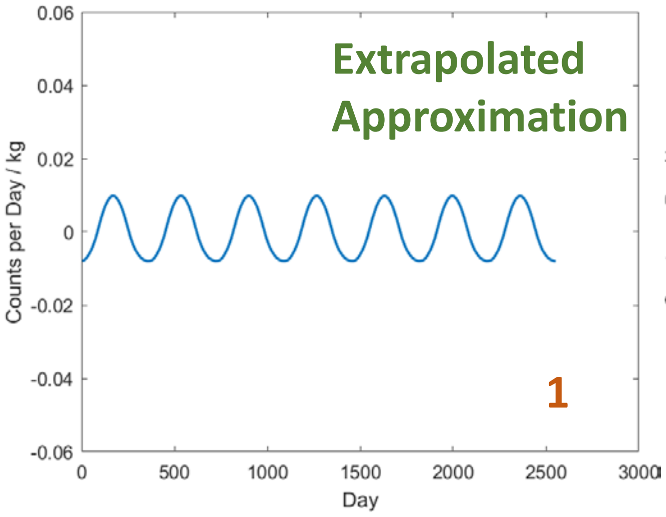

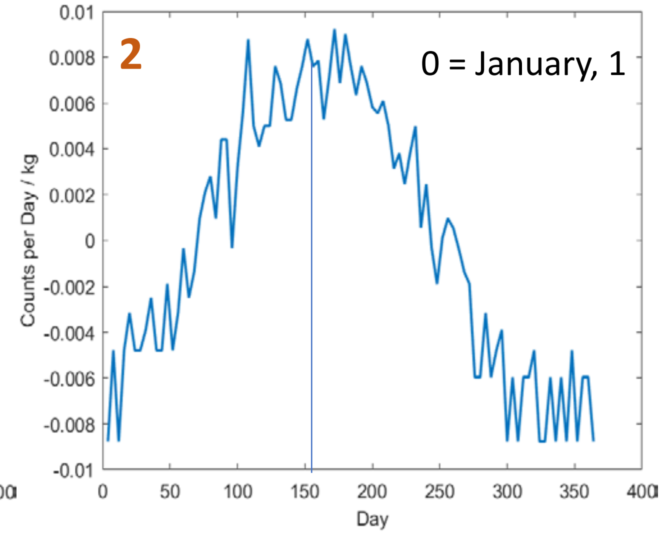

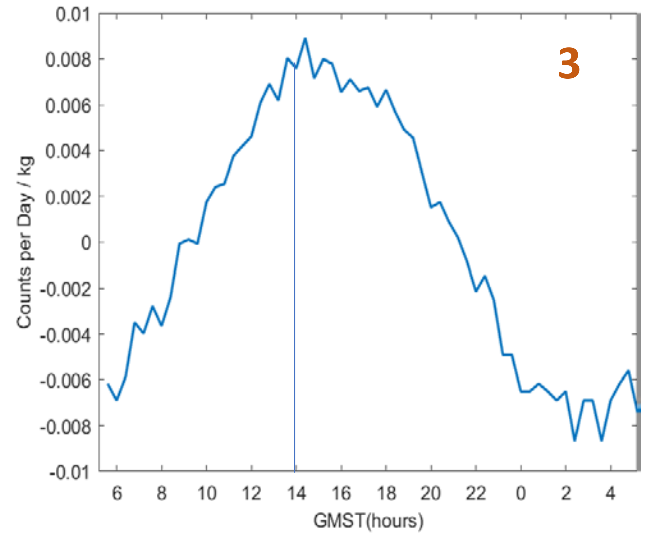

Fig.1. from Bernabei, R., Belli, P., Cappella, F. et al. Dark Matter: DAMA/LIBRA and its perspectives https://arxiv.org/abs/2209.00882

Experiment

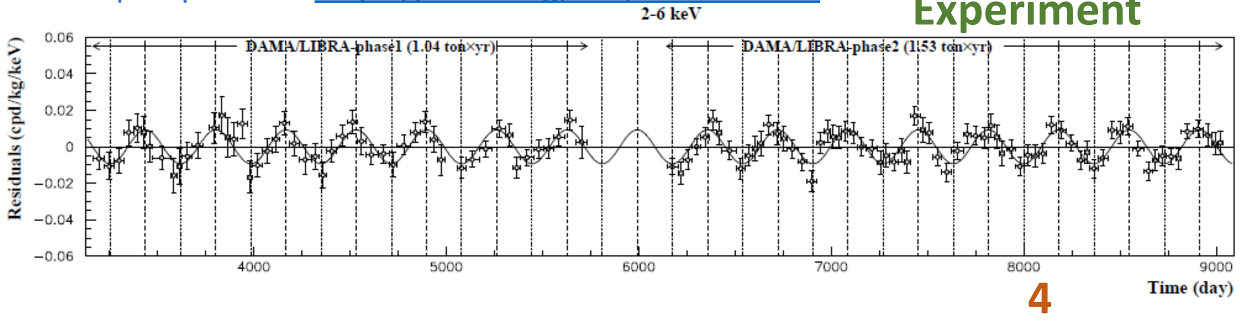

Figure 1: Experimental residual rate of the *single-hit* scintillation events measured by DAMA/LIBRA–phase1 and DAMA/LIBRA–phase2 in the (2–6) keV energy intervals as a function of the time. The superimposed curve is the cosinusoidal functional forms $A\cos\omega(t-t_0)$ with a period $T = \frac{2\pi}{\omega} = 1$ yr, a phase $t_0 = 152.5$ day (June 2^{nd}) and modulation amplitude, A, equal to the central value obtained by best fit. This figure is being reused from 20 .

Fig.1. from Bernabei, R., Belli, P., Cappella, F. et al. Model independent result on possible diurnal effect in DAMA/LIBRA-phase1. Eur. Phys. J. C 74, 2827 (2014).

Velocity

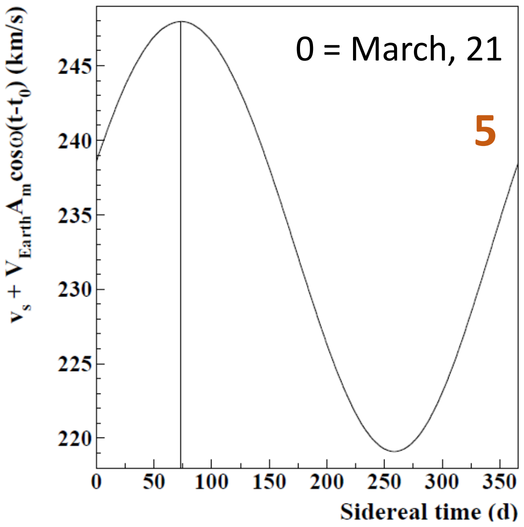

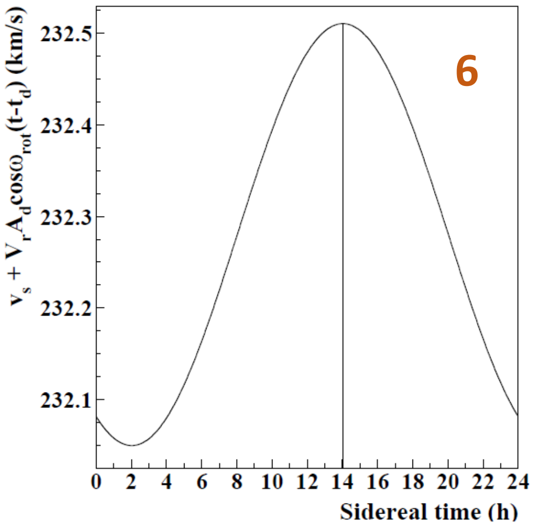

Distribution relative to the surface

- The proposed framework allows us to estimate the 3-dimensional spatial distribution of the flow of dark atoms, as well as track its change over time in the Earth's crust.

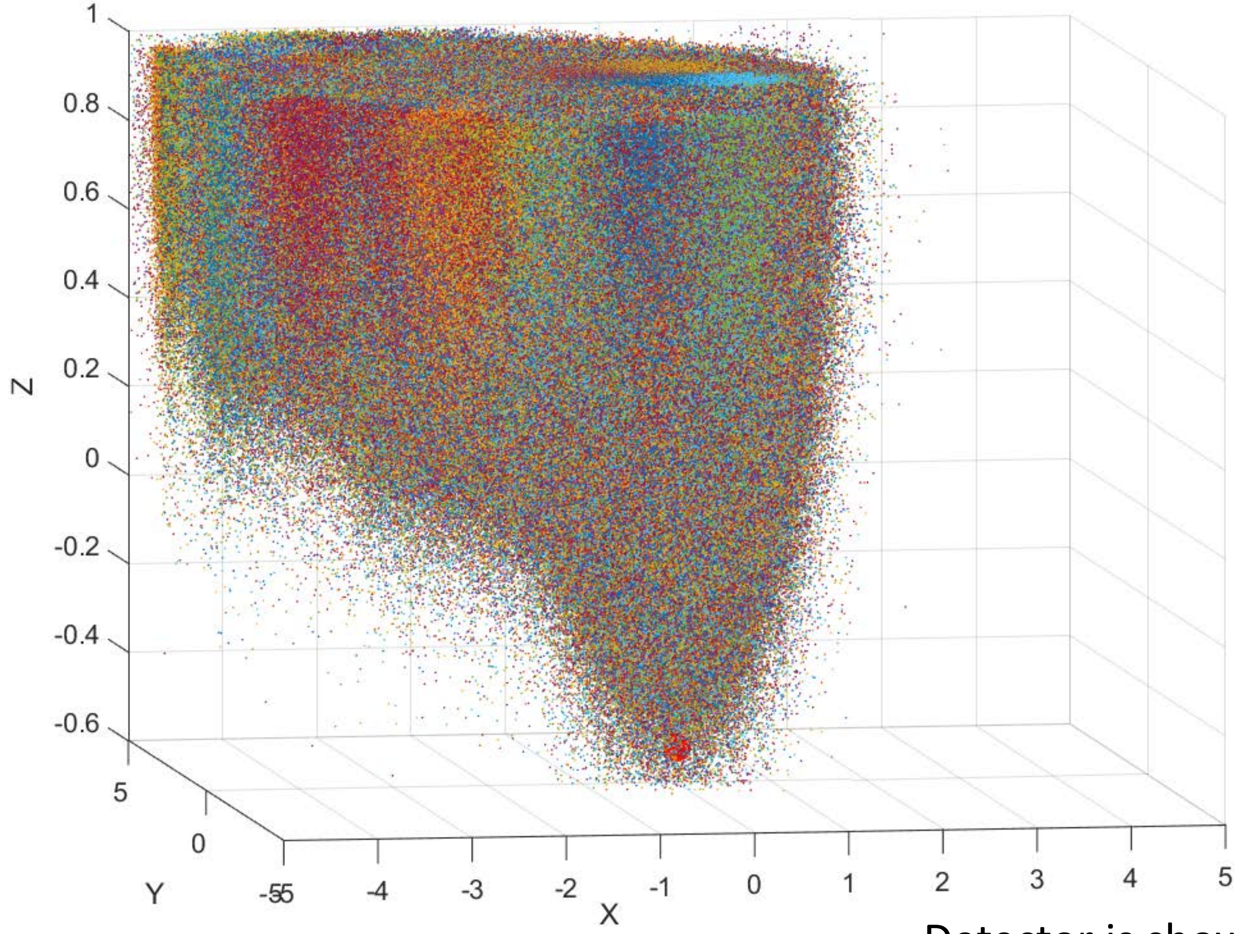

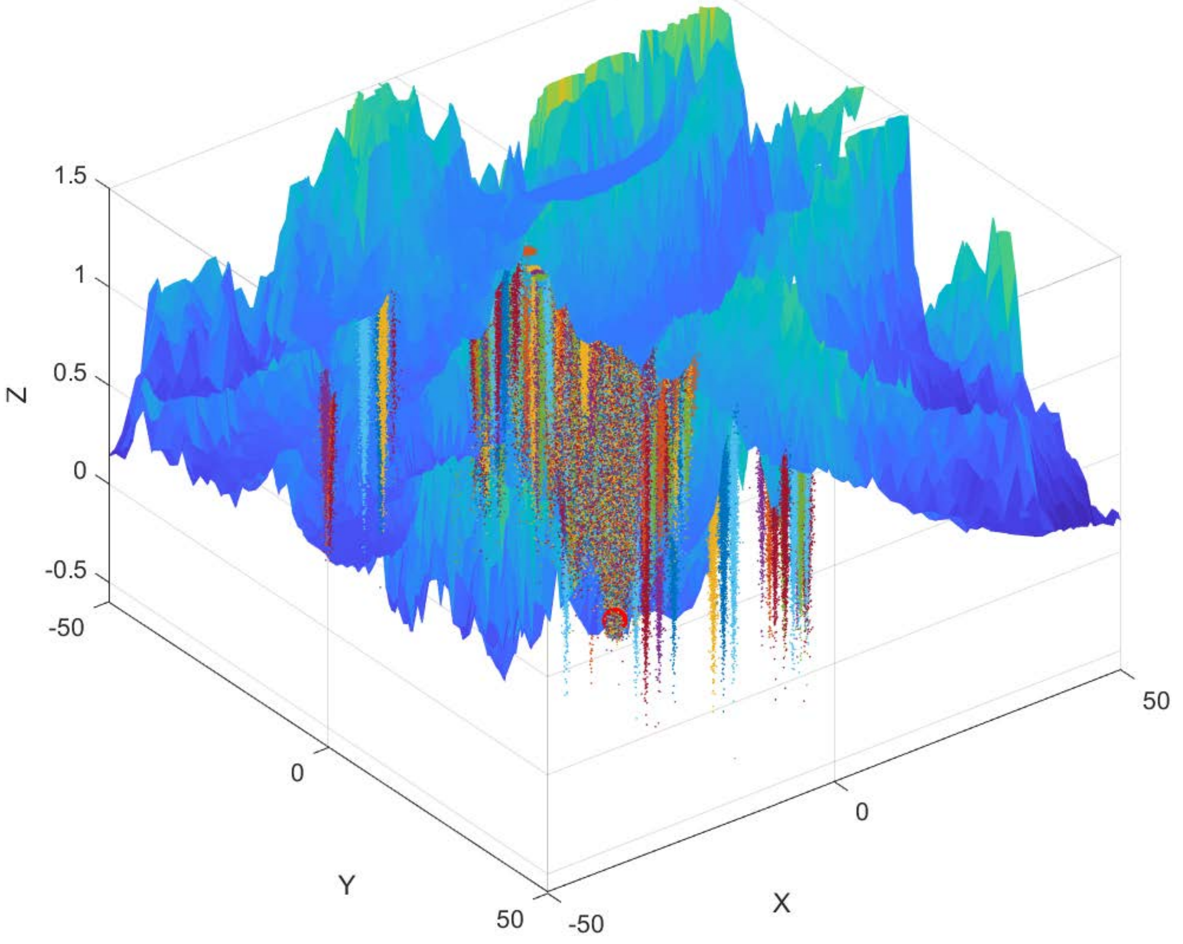

Detector is shown as a **red** dot.

Distribution near Detector

- Distribution can be calculated for an entire column or for a specific slice of the Earth's surface.
- Detector is shown as a **red** dot.
- The actual detector's geometry is a 3-dimentional parallelepiped.
- Very few particles actually get inside.

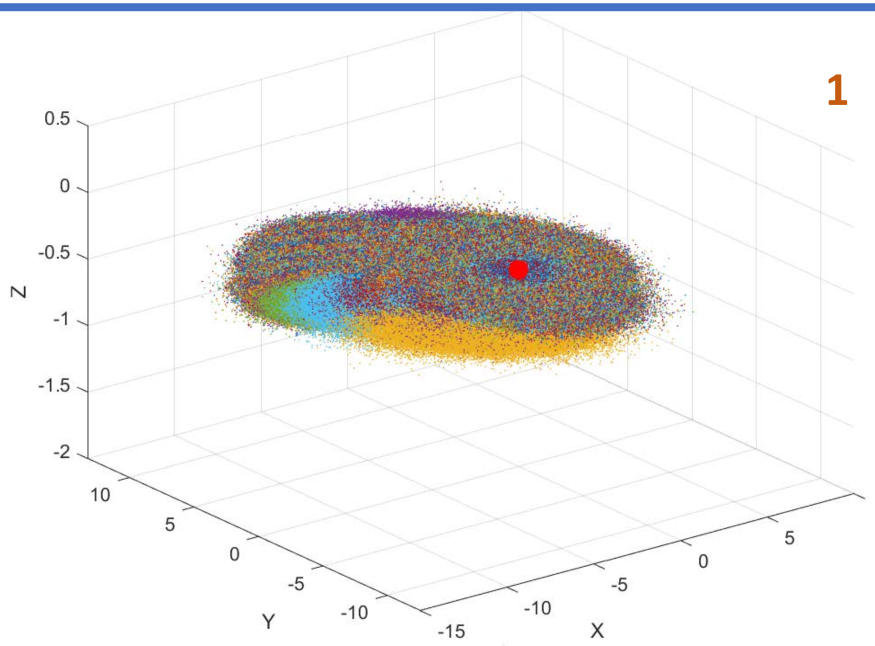

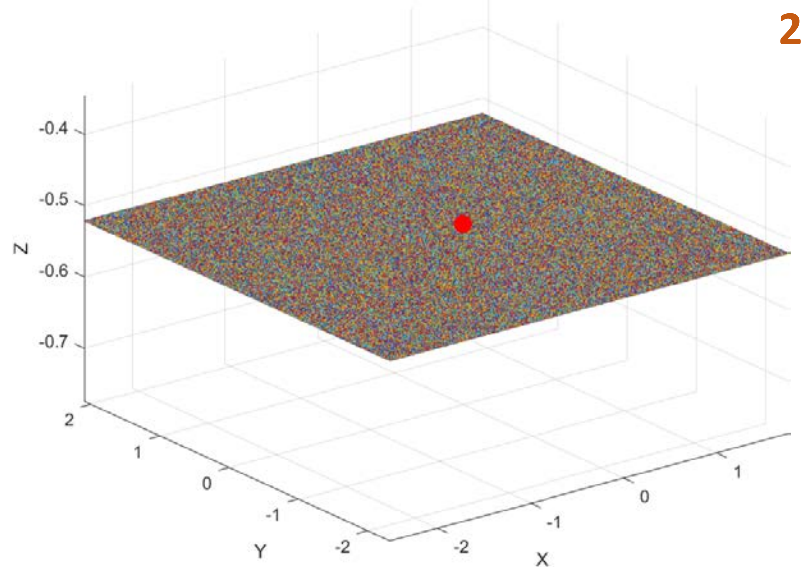

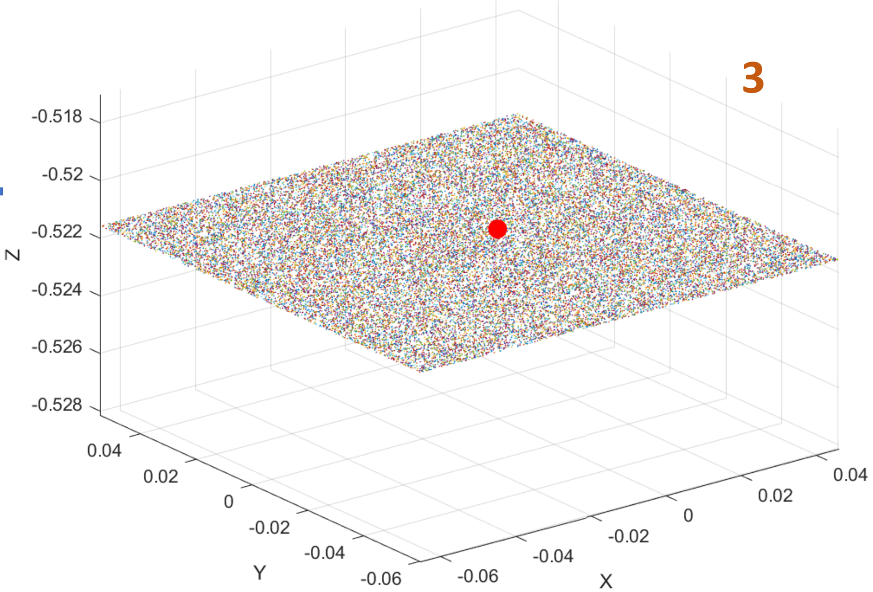

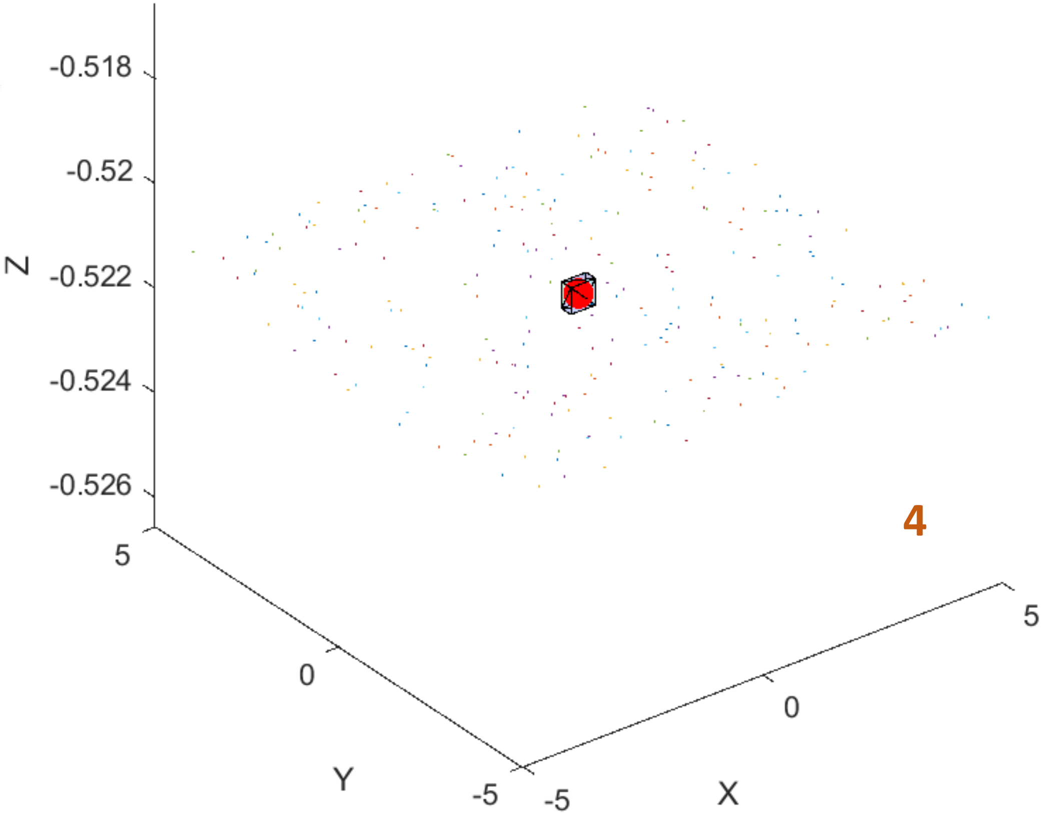

Conclusions

- A framework has been developed for modeling the processes of propagation and diffusion of dark atoms within the Earth's surface.
- The proposed model allows to estimate the concentration of dark atoms in underground detectors taking into account their geometry, underground depth and effects caused by the unevenness of the terrain above them, and the directions of particle arrival at the Earth's surface.
- Calculations are carried out with reference to real time, the Earth's orientation relative to the dark matter halo, the velocities and directions of motion of the Solar System and the Earth relative to the galactic center.
- The simulation shows the presence of daily and annual modulations, phase matches DAMA/LIBRA results and qualitative agreement in dynamics is observed.

References

1. R. Bernabei, P. Belli, V. Caracciolo, R. Cerulli, A. Di Marco, V. Merlo, F. Cappella, A. d'Angelo, A. Incicchitti, C.J. Dai, X.H. Ma, X.D. Sheng, F. Montecchia, Z.P. Ye, Dark Matter investigation with DAMA set-ups, Int. J. of Mod. Phys. A 37 (2022) 2240015 [doi:10.1142/S0217751X22400152]
2. R. Bernabei, P. Belli, A. Bussolotti, V. Caracciolo, F. Cappella, R. Cerulli, C.J. Dai, A. d'Angelo, N. Ferrari, A. Incicchitti, A. Leoncini, X.H. Ma, A. Mattei, V. Merlo, F. Montecchia, X.D. Sheng, Z.P. Ye, Further results from DAMA/LIBRA-phase2 and perspectives, Nucl. Phys. At. Energy 22 (2021) 329-342. [https://doi.org/10.15407/jnpae2021.04.329].
3. R. Bernabei, P. Belli, A. Bussolotti, F. Cappella, V. Caracciolo, R. Cerulli, C.J. Dai, A. d'Angelo, A. Di Marco, N. Ferrari, A. Incicchitti, X.H. Ma, A. Mattei, V. Merlo, F. Montecchia, X.D. Sheng, Z.P. Ye, The DAMA project: achievements, implications and perspectives. Prog. Part. Nucl. Phys. 114 (2020) 103810. [doi:10.1016/j.ppnp.2020.103810]
4. Khlopov, M. Y., Mayorov, A. G., Soldatov, E. Y. Composite Dark Matter and Puzzles of Dark Matter Searches. arXiv:1003.1144v1 [astro-ph.CO] 4 Mar 2010. https://doi.org/10.1142/S0218271810017962
5. L. P. Lifshitz, E. M.; Pitaevskii. Physical Kinetics, volume 10. Pergamon Press, 1981.
6. Bernabei, R., Belli, P., Cappella, F. et al. Model independent result on possible diurnal effect in DAMA/LIBRA-phase1. Eur. Phys. J. C 74, 2827 (2014). https://doi.org/10.1140/epjc/s10052-014-2827-1
7. Bernabei, R., Belli, P., d'Angelo, S. et al. Investigating Earth shadowing effect with DAMA/LIBRA-phase1. Eur. Phys. J. C 75, 239 (2015). https://doi.org/10.1140/epjc/s10052-015-3473-y
8. J. R. Cudell and M. Khlopov. Dark atoms with nuclear shell: A status review. International Journal of Modern Physics DVol. 24, No. 13, 1545007 (2015). https://doi.org/10.1142/S0218271815450078

THANK YOU FOR YOUR ATTENTION